RSC Advances

ROYAL SOCIETY OF CHEMISTRY

www.rsc.org/advances

What causes tumbling of *altro*-α-CD derivatives? Insight from computer simulations†

Ying Liu,[ab] Christophe Chipot,[cde] Xueguang Shao,[ab] and Wensheng Cai*[a]

[a]College of Chemistry, Research Center for Analytical Sciences, Tianjin Key Laboratory of Molecular Recognition and Biosensing, Collaborative Innovation Center of Chemical Science and Engineering, Nankai University, Tianjin 300071, People's Republic of China

[b]State Key Laboratory of Medicinal Chemical Biology, Nankai University, Tianjin, 300071, People's Republic of China

[c]Laboratoire International Associé Centre National de la Recherche Scientifique et University of Illinois at Urbana-Champaign, Unité Mixte de Recherche No. 7565, Université de Lorraine, B.P. 70239, 54506 Vandœuvre-lès-Nancy cedex, France

[d]Theoretical and Computational Biophysics Group, Beckman Institute, University of Illinois at Urbana-Champaign, Urbana, Illinois 61801, United States

[e]Department of Physics, University of Illinois at Urbana−Champaign, 1110 West Green Street, Urbana, Illinois 61801, United States

†Electronic supplementary information (ESI) available: Discussion on the physical origins of the free-energy barriers. Discussion on the steric constraints of the polyvinyl alcohol chain. Free-energy profiles that delineate the departure of a DMSO molecule from both rims of an *altro*-α-CD. Structural data of the alkyl *altro*-α-CD during tumbling.

* Address correspondence to wscai@nankai.edu.cn.

Abstract In water, a remarkable motion can be observed with a [2]rotaxane, wherein the rotor translocates by reeling its axle in the cavity of an *altro*-α-CD stopper. Similarly, in aqueous solution, an alkyl *altro*-α-CD dimer reels its alkyl chain in the *altro*-α-CD cavity to form a *pseudo*[1]rotaxane dimer. This reeling motion is in fact induced by the tumbling of the altropyranose unit of an *altro*-α-CD, a process shown to be solvent-dependent. Tumbling, however, does not occur in low-polarity solvents such as methanol and DMSO. In the present contribution, the mechanism that underlies solvent-controlled tumbling has been studied at the atomic level by means of molecular dynamics simulations combined with microsecond-timescale free-energy calculations. The free-energy profile delineating the tumbling in water of the altropyranose unit of an alkyl *altro*-α-CD indicates that a 19.8 kcal/mol barrier must be overcome to yield the self-inclusion complex, which is the most stable state available to the supramolecular assembly. In DMSO, the free-energy barrier is about 21.0 kcal/mol higher, and the self-included alkyl *altro*-α-CD corresponds to a metastable state. These results provide new thermodynamic and kinetic insights into solvent-controlled tumbling, and reveal the essence of different experimental observations. Further investigation shows that aside from the polarity of solvent, tumbling of the *altro*-α-CD derivative stems from the hydrophobicity of the side chain and the propensity of the former to include the latter, which opens perspectives for the design of new, related supramolecular assemblies.

Keywords altropyranose · self-inclusion · free-energy calculation · tumbling · water · DMSO · solvent effect

Introduction

Rotaxanes and pseudorotaxanes are mechanically coupled molecular architectures formed by a linear axle and a cyclic molecule threaded onto the latter. The cyclic molecule, commonly known as the "wheel", can shuttle under external stimuli between the stations of the axle in a controlled and repeatable fashion. Based on this unique property, rotaxanes and pseudorotaxanes can be utilized in a wide range of applications relevant to many research areas, including molecular recognition,[1] drug delivery,[2] design of molecular motors and switches,[3] as well as other artificial molecular machines.[4,5] Macrocyclic molecules, such as crown ethers, calixarenes, cucurbiturils, pillararenes and cyclodextrins (CDs), often function as wheels in the context of rotaxanes and pseudorotaxanes.[6-10] To control the molecular movement of the wheel spinning about its axle, temperature, pH, chemicals, electrons, photons, and solvent are usually expected to act as stimuli.[11-16]

A novel [2]rotaxane, designed and synthesized by Harada and co-workers,[17] is composed of an α-CD wheel, a decamethylene (C10) chain, a stilbene unit and an *altro*-α-CD stopper containing one altropyranose unit and five glucopyranose units (see Fig. 1A). This [2]rotaxane is essentially solvent dependent, that is, in dimethylsulfoxide (DMSO), the α-CD wheel includes the C10 chain, and it further translates to also embrace the stilbene group when DMSO is replaced by water. Two-dimensional ROESY NMR measurements have elucidated that in an aqueous solution, the altropyranose unit of the *altro*-α-CD stopper tends to rotate about an α(1,4) bond, concomitant with the isomerization from $^1C_4$ to $^4C_1$ (see Fig. 1C), thus forming a self-inclusion complex. Tumbling of the altropyranose unit leads to reeling of the C10 chain into the *altro*-α-CD cavity, hence pushing the α-CD wheel onto the stilbene group. Reeling of the axle into the host molecule, however, was not observed in DMSO, implying that tumbling of the altropyranose unit cannot occur under such circumstance.

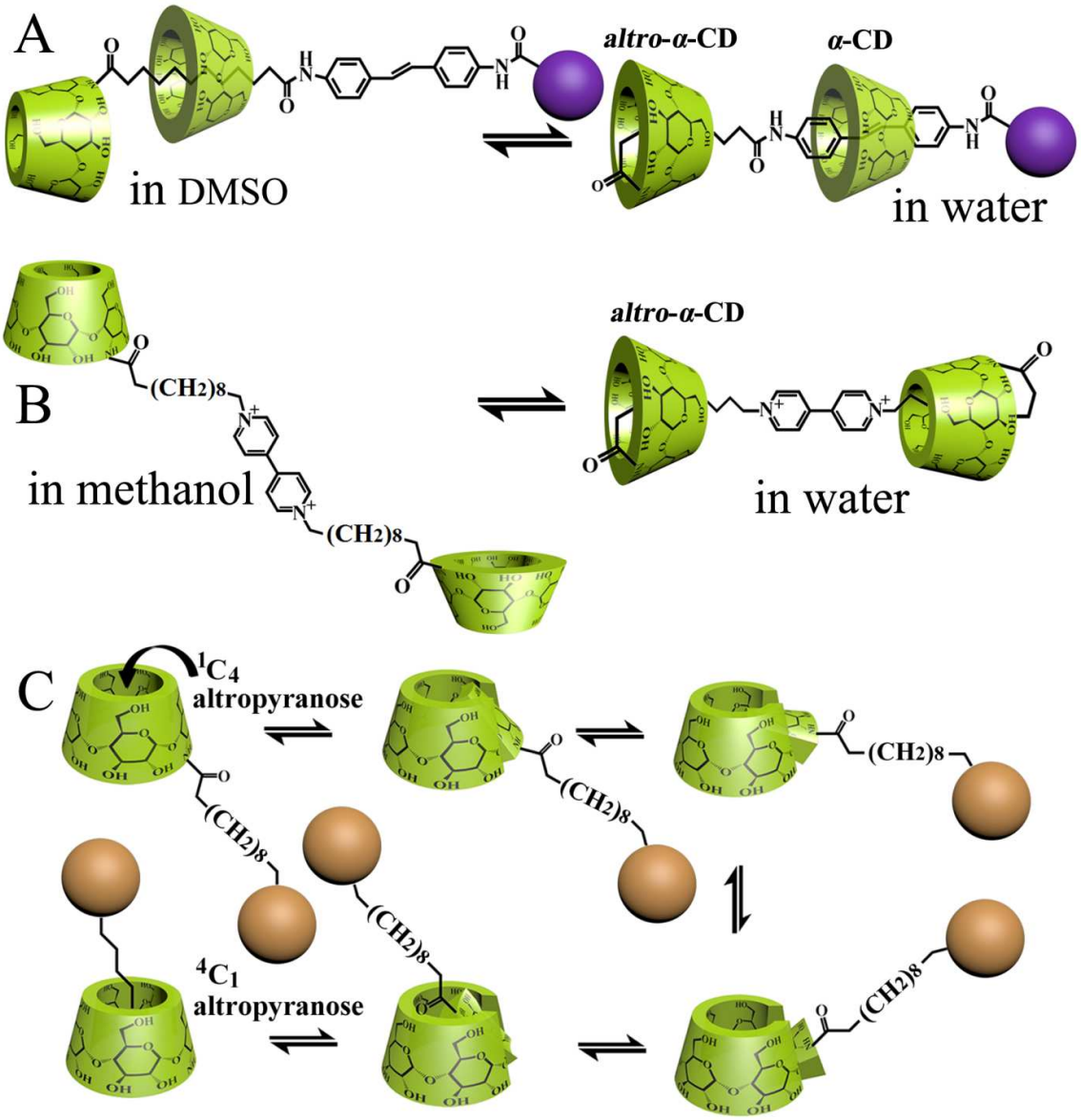

Fig. 1 (A) Representative configurations of the [2]rotaxane, wherein the *α*-CD wheel shuttles along the axle in response to the tumbling of the altropyranose unit. (B) Formation of the *pseudo*[1]rotaxane dimer from the alkyl *altro*-*α*-CD dimer via tumbling of the altropyranose units. (C) Schematic illustration of the tumbling of an altropyranose unit.

Moreover, Harada et al.[18] synthesized an *altro*-*α*-CD dimer with two C10 linkers and a viologen unit (see Fig. 1B). Of particular interest, this *altro*-*α*-CD dimer converts spontaneously to a *pseudo*[1]rotaxane dimer in water. ^{1}H NMR spectra reveal that the formation of the

pseudo[1]rotaxane dimer results from tumbling of the altropyranose units connecting to the C10 linkers, as shown in Fig. 1C. Similar to the above-mentioned [2]rotaxane, this tumbling process is found to be very solvent dependent. Replacing water by methanol of lower polarity disables the transformation.

It is obvious that tumbling of the altropyranose unit plays a critical role in the shuttling of the [2]rotaxane and in the formation of the *pseudo*[1]rotaxane dimer (see Fig. 1). We have shown in a preliminary investigation[19] that the self-inclusion of an *altro*-*α*-CD derivative stems from tumbling of its altropyranose unit rather than threading of its bulky end group. The estimated free-energy change characterizing tumbling of the altropyranose unit of a mono-*altro*-*α*-CD in aqueous solution was found close to the experimentally measured quantity. The main thrust of the present contribution is to examine the effects that the solvent exerts on the tumbling process. Toward this end, an alkyl *altro*-*α*-CD model was constructed as a paradigm for the study of solvent-dependent tumbling.

Using this model, all-atom molecular dynamics (MD) simulations combined with free-energy calculations have been performed. The potentials of mean force (PMFs) characterizing the tumbling process in water and DMSO were determined. The interaction of the alkyl chain with both the solvent and the *altro*-*α*-CD was analyzed to shed new light onto the physical origin of tumbling.

Methods

Molecular models. To assess the effect of the solvent on the tumbling of the altropyranose unit, an alkyl *altro*-*α*-CD model, formed by an *altro*-*α*-CD, a C10 linker and a viologen unit which connects with a methyl group, was constructed as described in Fig. 2A:**1**. Besides, to evaluate how the hydrophobicity of the chain influences tumbling, a very similar molecular model was constructed, replacing the C10 chain by a hydrophilic polyvinyl alcohol chain (see Fig. 2A:**2**). The

geometry of these two molecules was optimized using a conjugate-gradient algorithm. The $^1C_4$ chair conformation was chosen for the initial conformation for the altropyranose unit. The alkyl *altro*-*α*-CD and the polyvinyl alcohol *altro*-*α*-CD were subsequently immersed in a box of water, on the one hand, and in a box of DMSO, on the other hand, thus, resulting in four separate molecular assemblies. Two chloride ions were placed in each solvent box to ensure electric neutrality. For each solvated system, a 10-ns equilibrium MD simulation was performed prior to subsequent free-energy calculations.

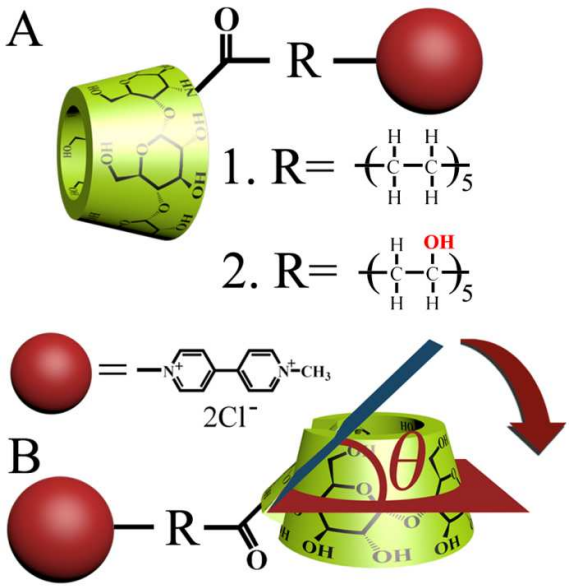

Fig. 2 (A) Molecular model of the alkyl *altro*-*α*-CD formed by an *altro*-*α*-CD, a C10 linker and a viologen unit connected to a methyl group (1), and of the polyvinyl alcohol *altro*-*α*-CD formed by an *altro*-*α*-CD, a polyvinyl alcohol linker and a viologen unit connected to a methyl group (2). (B) Schematic representation of the transition coordinate, θ. To describe the continuous tumbling process, the transition pathway spans $-300° \leq \theta \leq +100°$.

Molecular dynamics simulations. All the atomistic MD simulations described herein were

performed using the parallel, scalable MD program NAMD 2.10[20] with the CHARMM 36 force field. A number of parameters describing the side chain, which are absent in this force field, were optimized in a previous study.[21] The q4md-CD force field,[22] an Amber-derived force field, has been shown to perform remarkably well for the modeling of CDs.[23,24] However, owing to possible inconsistencies between the CHARMM36 and the q4md-CD force fields — arising from distinct parameterization philosophies, the CHARMM force field for carbohydrates,[25,26] which has proven suitable for the study of CDs,[19,21] was employed in this work to describe the pyranose monosaccharides and glycosidic linkages of the *altro*-α-CD. The TIP3P model was used for water,[27] alongside the all-atom DMSO model proposed by Strader and Feller.[28] The latter additive model offers a reasonable reproduction of the experimental dielectric constant of the liquid. The temperature and the pressure were maintained at 288 K and 1 atm, respectively, using Langevin dynamics and the Langevin piston method.[29] Covalent bonds involving hydrogen atoms were constrained to their equilibrium length by means of the SHAKE/RATTLE algorithm,[30,31] except for water molecules, for which the SETTLE algorithm was applied.[30] Long-range electrostatic forces were evaluated using the particle mesh Ewald scheme,[32] and a smoothed 12 Å spherical cutoff was used to truncate short-range van der Waals and electrostatic interactions. The r-RESPA multiple time-step algorithm[33] was applied to integrate the equations of motion with a time step of 2 and 4 fs for short- and long-range interactions. Visualization and analysis of MD trajectories were carried out with the VMD package.[34]

Free-energy calculations. The free-energy profiles that characterize tumbling in the two different solvents were generated using the multiple-walker adaptive biasing force (MW-ABF) algorithm,[35,36] an improved importance-sampling approach aimed at achieving ergodic sampling on

the basis of the ABF algorithm[37-41] implemented within the collective variables module[42] of NAMD. In MW-ABF calculations, nine walkers were spawned and the force samples accrued by each walker were combined every 1,000 steps. The transition coordinate, θ, was defined as the dihedral angle between the altropyranose unit bearing the side chain and the plane formed by the six glycosidic oxygen atoms of the *altro*-*α*-CD (see Fig. 2B). It has been demonstrated in a previous work[19] that the collective variable used herein represents a suitable transition coordinate for exploring the tumbling of a monomer in a cyclic oligomer. In order to describe the complete and continuous tumbling, the transition pathway being explored spanned $-300° \leq \theta \leq +100°$, wherein the interval between −300° and −180° corresponds to that between +60° and +180°. The backbone of the *altro*-*α*-CD was softly restrained, except for the altropyranose unit connecting the side chain, which was left to rotate freely. The instantaneous values of the force were stored in 1° wide bins. Four independent MW-ABF simulations, corresponding to the alkyl *altro*-*α*-CD and the polyvinyl alcohol *altro*-*α*-CD immersed in water and in DMSO, were carried out. The total simulation time amounted to 0.54 μs, 1.21 μs, 1.10 μs and 1.28 μs, respectively. Block average regression[39,40,43] was applied to estimate the standard error of the free-energy change.

Results

Free-energy profiles. The calculated free-energy profiles characterizing the tumbling of the alkyl *altro*-*α*-CD in water and DMSO have been gathered in Fig. 3. The structures corresponding to the points of inflection, from A to F in the PMFs, are shown in Fig. 4A-F. In the initial structure of the alkyl *altro*-*α*-CD for both models, the alkyl chain stretches freely outside the CD cavity, and the dihedral angle, θ, is measured to be +75°, wherein the altropyranose adopts a $^1C_4$ chair conformation. The horizontal arrows in Fig. 3 denote the evolution of the dihedral angle as the alkyl chain is

included into the CD cavity.

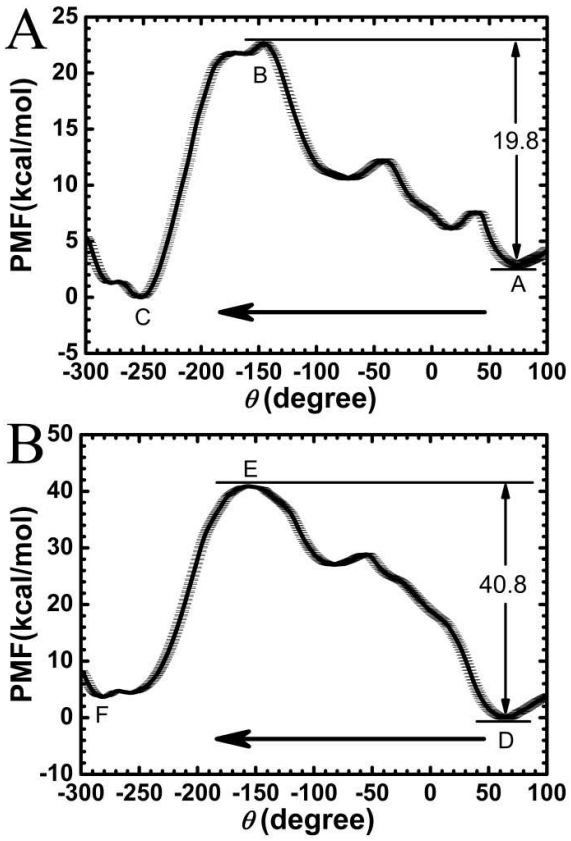

Fig. 3 Free-energy profiles delineating the tumbling of the altropyranose monomer of the alkyl *altro*-*α*-CD along the transition coordinate, *θ*, defined in Fig. 2: (A) in water, and (B) in DMSO. The values of the dihedral angle corresponding to points of inflection A to F of the PMFs are +75°, −145°, −253°, +65°, −155° and −280°, respectively. The error bars correspond to the statistical error of the free-energy calculation, i.e., the precision.

A closer look at the PMF of Fig. 3A reveals that the profile possesses two minima separated by a 19.8 kcal/mol free-energy barrier, which is in close agreement with the experimental activation free energy (ca. 21.0 kcal/mol).[17,18] There are several common factors contributing to the free-energy barriers both in water and in DMSO, including (1) the inevitable isomerization of the altropyranose

unit and its two neighboring glucopyranose units, (2) the deformation of the CD, (3) the desolvation of the side chain, (4) breaking hydrogen bonds at the secondary side of the CD, and (5) the unfavorable interaction of the hydroxyl groups of the altropyranose unit with the hydrophobic cavity. The latter two factors also constitute the main barrier in the tumbling of the altropyranose unit of a mono-*altro*-*α*-CD, as was reported previously.[19] A detailed discussion can be found in the ESI†.

The structure in Fig. 4A, corresponding to a local minimum of the PMF (namely, point A, θ = +75°), is very similar to the initial conformation of the alkyl *altro*-*α*-CD. As the dihedral angle, θ, approaches −145°, the PMF reaches its maximum at point B. It can be observed in Fig. 4B that the alkyl chain translocates from the secondary side of the *altro*-α-CD to its primary side and is nearly enclosed into the CD cavity. The structure of the global minimum of the PMF (at point C, $\theta = -253°$) corresponds to the final self-inclusion complex, wherein the alkyl chain is included in the CD cavity and the altropyranose isomerizes into the metastable $^4C_1$ chair conformation. Meanwhile, the viologen unit resides over the narrower rim of the *altro*-*α*-CD (see Fig. 4C).

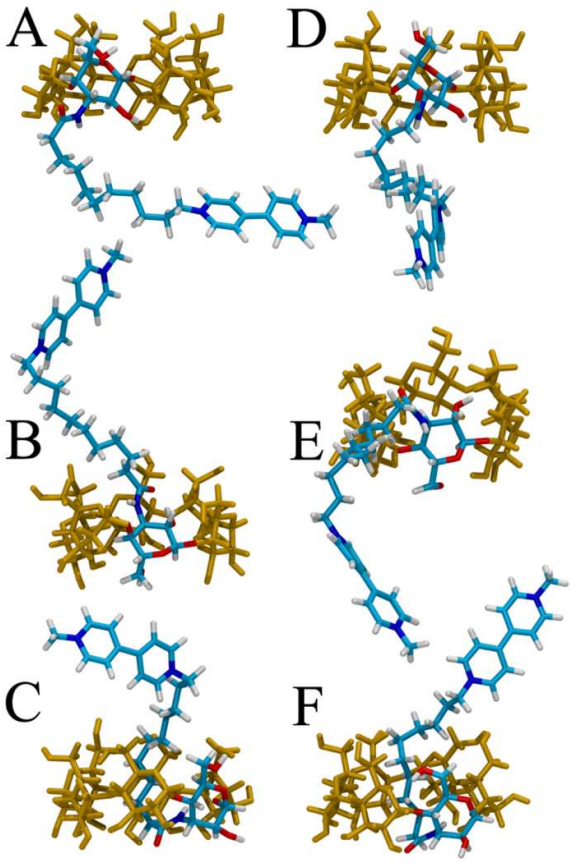

Fig. 4 Conformations of the alkyl *altro*-*α*-CD at the points of inflection of the PMFs. (A) When $\theta \simeq +75°$, the altropyranose unit adopts a $^{1}C_{4}$ chair conformation. (B) When $\theta \simeq -145°$, the alkyl chain is nearly enclosed in the cavity of the *altro*-*α*-CD and the altropyranose unit shows a twist-boat conformation. (C) When $\theta \simeq -253°$, the alkyl chain is included in the CD cavity and the altropyranose unit isomerizes into a $^{4}C_{1}$ chair conformation. (D) When $\theta \simeq +65°$, the altropyranose unit adopts a $^{1}C_{4}$ chair conformation. (E) When $\theta \simeq -155°$, the altropyranose unit shows a twist-boat conformation. (F) When $\theta \simeq -280°$, the altropyranose unit is in a $^{4}C_{1}$ chair conformation. Water and DMSO molecules are omitted for clarity. The corresponding coordinate files can be found in ESI†.

However, the self-included alkyl *altro*-*α*-CD in DMSO (see Fig. 4F) corresponds here to the local minimum of the PMF (i.e., point F, where $\theta = -280°$), while the structure of the global minimum (i.e., point D, where $\theta = +65°$) is characterized by the alkyl chain protruding outside the

CD cavity, as shown in Fig. 4D. The barrier of the PMF reflects an unstable state, wherein the altropyranose unit adopts a twist-boat conformation and the hydrophobic alkyl chain stretches to the bulk DMSO (see Fig. 4E). The PMF determined in DMSO features a 40.8 kcal/mol barrier (see Fig. 3B), which is significantly higher than that in water, hence suggesting that the self-inclusion of the alkyl chain into the *altro*-*α*-CD cavity, which derives from tumbling of the altropyranose unit, is very unlikely to happen spontaneously in DMSO, at room temperature.

Moreover, it is noteworthy that in water, the free energy of the self-inclusion state of the alkyl *altro*-*α*-CD, which corresponds to the global minimum of the PMF (at point C in Fig. 3), is about 2.9 kcal/mol lower than that of the non-inclusion state prior to tumbling (at point A). The non-included alkyl *altro*-*α*-CD evolves toward the thermodynamically stable state of the self-inclusion structure through tumbling of the altropyranose unit. In stark contrast, in DMSO, the free energy of the self-included alkyl *altro*-*α*-CD is higher by 3.7 kcal/mol than that of the non-inclusion one, hence implying that tumbling in DMSO is thermodynamically impossible.

Conformational transition of the altropyranose unit. The conformational transition of the altropyranose unit during tumbling was analyzed for both molecular assemblies using a conformation coordinate, ε,[44,45] expressed as

$$\varepsilon = \frac{1}{6}(\tau_1 \quad \tau_2 \mid \tau_3 \quad \tau_4 \cdot \tau_5 \quad \tau_6) \tag{1}$$

where the τ_i are the six internal dihedral angles of the altropyranose ring depicted in Scheme 1. The two isomeric forms of the chair conformation of the altropyranose unit, that is $^1C_4$ and $^4C_1$, correspond to values of ε approximately equal to +60° and −60°, while the boat-like intermediate approximately corresponds to a value of ε of 0°.[44,45]

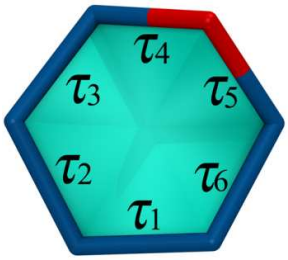

Scheme 1. Schematic illustration of the six internal dihedral angles in an altropyranose unit.

Using this conformation, we are able to observe the conformational transition of the altropyranose unit, namely $^{1}C_{4}$ chair to boat-like to $^{4}C_{1}$ chair. As can be seen in Fig. 5A and B, ε varies from ca. +60° to ca. −60° as tumbling proceeds, indicative of the isomerization of the altropyranose unit from $^{1}C_{4}$ chair to $^{4}C_{1}$ chair via a boat-like intermediate, in line with the experimental results based on ^{1}H NMR and 2D ROESY NMR spectra.[17,18]

Furthermore, as can be seen in Fig. 5, conformation coordinate ε exhibits a different behavior, compared to transition coordinate θ. In water, the altropyranose adopts a boat conformation for most values of θ, while it does not in DMSO. This discrepant behavior can be ascribed to the formation of hydrogen bonds. It can be observed in Fig. 6B that the hydrogen bonds formed within the CD in DMSO outnumber those in water when tumbling begins (the region of $-50° < \theta < +100°$). The relatively strong hydrogen-bonding network in DMSO results in a greater rigidity of the CD, which may thwart isomerization of the altropyranose unit into the boat conformation. In contrast, in the range of $-200° < \theta < -150°$, the number of hydrogen bonds formed within the CD in DMSO is lesser than that in water (see Fig. 6B), which confers to the CD a greater flexibility, hence facilitating isomerization from boat to $^{4}C_{1}$ chair conformation. As a consequence, the population of boat conformations in the course of tumbling is lower in DMSO than in the aqueous solution.

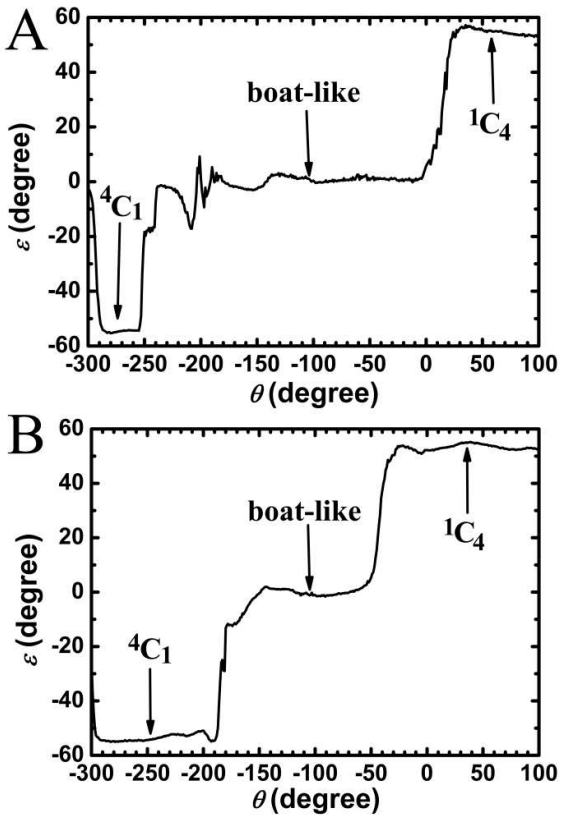

Fig. 5 Conformational transition of the altropyranose unit of the alkyl *altro*-*α*-CD in (A) water, and (B) DMSO, based on the ε conformation defined in equation 1.

Intermolecular and intramolecular hydrogen bonds. Hydrogen bonds are considered to be important structural features in the course of tumbling. To appreciate the stark contrast between the free-energy barriers determined in water and DMSO, the hydrogen bonds formed within the CD and those formed between the CD and the solvent molecules were examined. As can be seen in Fig. 6A, both water and DMSO molecules are engaged in the formation of intermolecular hydrogen bonds. Since water acts both as a hydrogen-bond donor and as a hydrogen-bond acceptor, while DMSO only acts as an acceptor, intermolecular hydrogen bonds involving water clearly outnumber those formed with DMSO (see Fig. 6A). It follows that one expects the strength of the hydrogen-bonding network of CD to be markedly weakened in water, compared to what it would be in DMSO, as it is

confirmed in Fig. 6B. Furthermore, as can be observed in the region of $-150° < \theta < +100°$, the quantity of hydrogen bonds in water is perceptibly less than that in DMSO. The relatively weak hydrogen-bonding network within the CD results in a lower free-energy barrier. Put together, the marked propensity of water towards hydrogen bonding contributes to the spontaneous occurrence of tumbling in water.

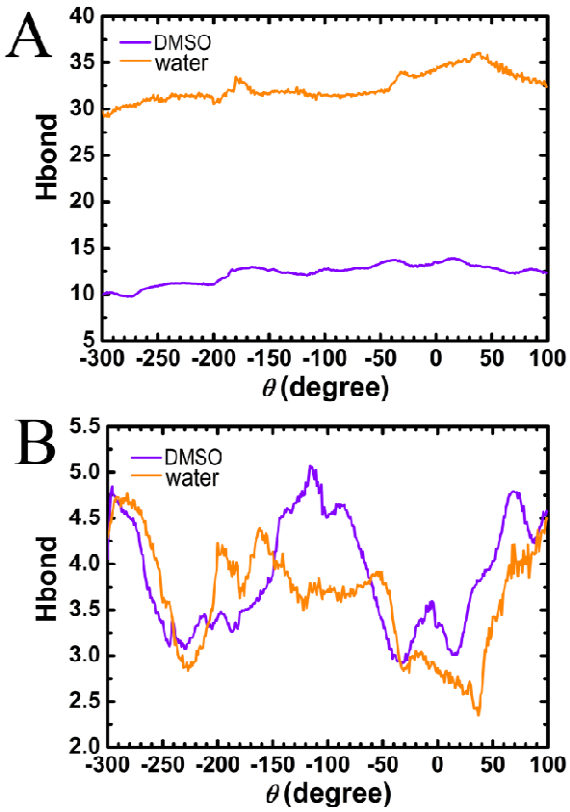

Fig. 6 Evolution of the average number of (A) intermolecular hydrogen bonds formed between the CD and the solvent molecules, and (B) intramolecular hydrogen bonds within the CD, in water and DMSO. The hydrogen-bonding criteria are (i) the angle O–H···O > 135° and (ii) the distance O···O < 3.5 Å.

Solvent molecules within the CD cavity. To interpret further the much higher free-energy barrier in DMSO, the influence of solvent molecules on tumbling has been explored. It has been

observed from the MD trajectories that the non-included alkyl *altro*-*α*-CD is inclined to bind a DMSO molecule at each rim (see Fig. 7A), which may constitute an obstacle to the tumbling of the altropyranose unit. In light of this observation, the residence time of the solvent molecules near the primary and the secondary rim of the CD has been estimated on the basis of a 10-ns equilibrium simulation. Here, the residence time of a solvent molecule is defined as the time interval between two adjacent configurations multiplied by the number of continuous configurations in which this solvent molecule is present. Longer residence time implies lesser mobility. Fig. 8 indicates that, compared to water, DMSO molecules reside in both rims of the CD for longer periods of time, which can be explained by its suitable size to snug in the cavity of the CD. The free-energy profiles delineating the departure of a DMSO molecule from both rims of an *altro*-*α*-CD (see the ESI†) suggest that the *altro*-*α*-CD cavity has two binding sites for DMSO, at each rim of the macrocycle. The stable binding of DMSO molecules to the CD entails a lower mobility of the former, hindering the tumbling of the altropyranose unit and penetration of the chain into the cavity.

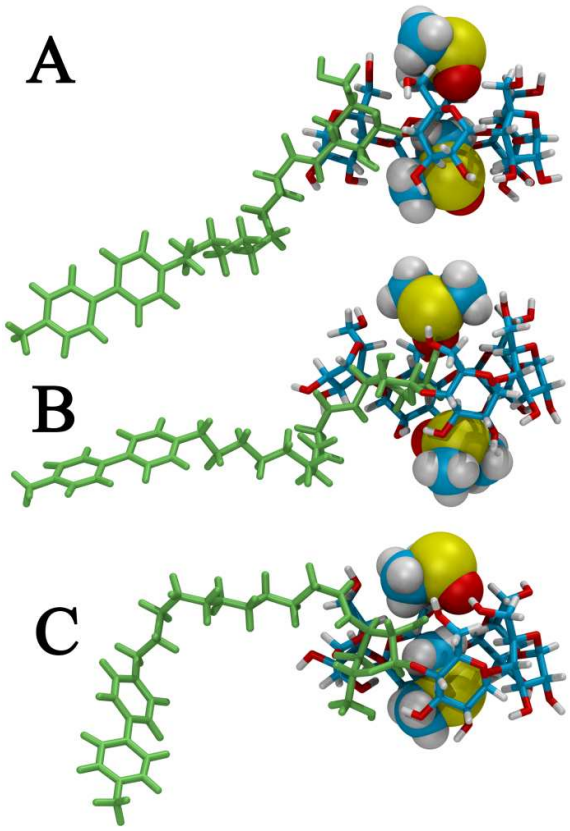

Fig. 7 Snapshots of the alkyl *altro*-*α*-CD with the encapsulated DMSO molecules at (A) $\theta = +65°$, (B) $\theta = -50°$ and (C) $\theta = -155°$, obtained from the MD trajectories of tumbling.

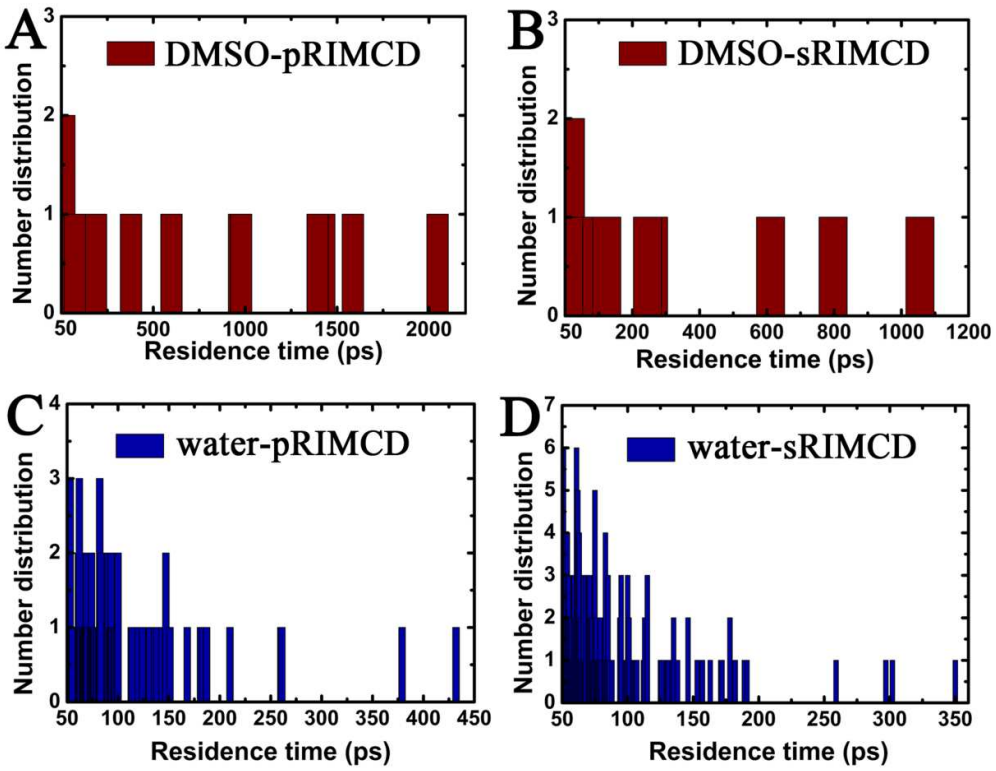

Fig. 8 Number distribution of DMSO molecules that reside at (A) the primary rim, and at (B) the secondary rim of the CD. Number distribution of water molecules that reside at (C) the primary rim, and at (D) the secondary rim of the CD. The results were inferred from an independent 10-ns MD trajectory.

Spontaneous binding of two DMSO molecules to the CD was also observed in the tumbling process prior to the inclusion of the chain, as can be seen in Fig. 7B and C, even when the altropyranose unit tumbled to the center of the CD cavity. These bound DMSO molecules constitute steric hindrances for the tumbling of the altropyranose unit and the threading of the chain, and, hence, contribute significantly to the free-energy barrier in DMSO. Water molecules with greater mobility will, however, not be trapped in the CD cavity, thereby rationalizing qualitatively the much lower free-energy barrier in water.

Solvation and solvent-accessible surface area. The distribution of the solvent molecules around the alkyl chain and the viologen unit was monitored in the course of tumbling by computing the bidimensional radial distribution functions, $g(r; \theta)$, of the oxygen atom of water or the sulfur atom of DMSO with respect to the centroid of the alkyl chain (Fig. 9A and B) and the viologen unit (Fig. 9C and D). By doing so, valuable structural information about the local concentration of water and DMSO molecules around the alkyl chain and the viologen unit is obtained, allowing the corresponding solvation shells to be visualized. As can be seen in Fig. 9, the maximum of the density found in the region spanning $4 \leq r \leq 6$ Å coincides with the first solvation shell of the alkyl chain or the viologen unit. In Fig. 9A and B, a solvation shell is formed for the alkyl chain when $-200° \leq \theta \leq +100°$. When θ is comprised between −300° and −200°, no solvation shell is observed — in other words, the solvation shell of the alkyl chain is disrupted as the alkyl chain enters the cavity of the *altro*-α-CD. Since the alkyl chain is hydrophobic, its desolvation from bulk water is extremely favorable. As a result, the self-included alkyl *altro*-α-CD in water is more stable than its non-included counterpart (see Fig. 3A). In contrast, DMSO is a polar, aprotic solvent, the polarity of which is weaker than that of water — solvophobic effects in DMSO are, therefore, not as pronounced as those in water. It follows that the alkyl chain tends to stay in the bulk of DMSO, rather than enter the CD cavity (see Fig. 3B). In Fig. 9C and D, the solvation shell of the viologen unit is continuous along θ, hence suggesting that the viologen unit never accesses the CD cavity during the self-inclusion of the alkyl chain.

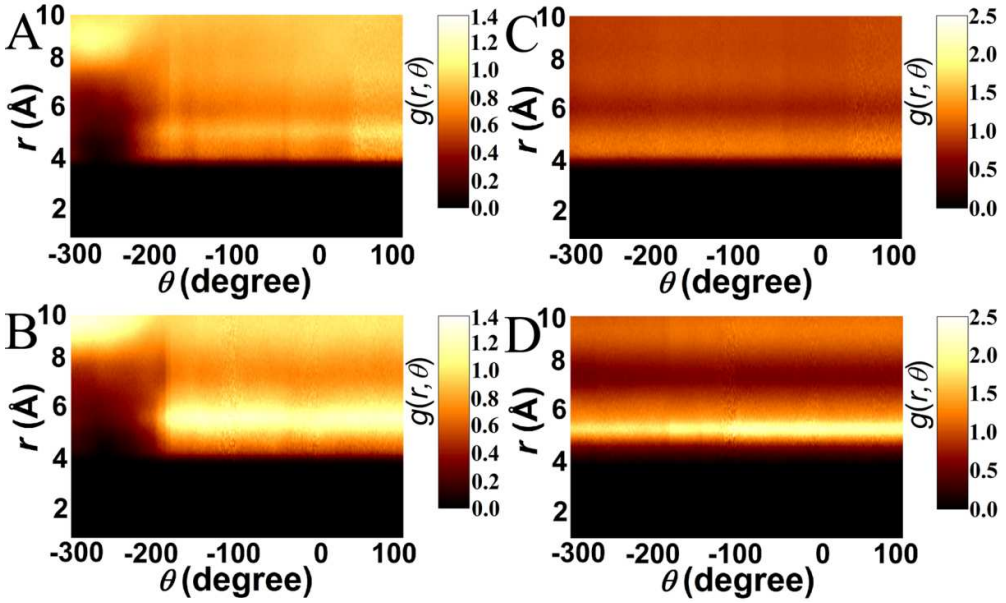

Fig. 9 Evolution of the radial distribution function of the centroid of the alkyl chain–water oxygen/DMSO sulfur pair as a function of *r*, the distance separating the pair of atoms, for the tumbling (A) in water, and (B) in DMSO. Evolution of the radial distribution function of the centroid of the viologen unit–water oxygen/DMSO sulfur pair as a function of *r* for tumbling (C) in water, and (D) in DMSO.

The solvent-accessible surface area (SASA) of the alkyl chain during tumbling in both water and DMSO has also been measured. As can be observed in Fig. 10, the SASA of the alkyl chain gradually decreases as tumbling proceeds, and reaches in water a minimum at about −250°. This minimum coincides with the global minimum of the PMF determined in the aqueous environment (see Fig. 3A). Yet, the SASA of the alkyl chain in DMSO remains unchanged in the region of −150° < θ < +100°, thus indicating that the alkyl chain tends to stay in DMSO, instead of entering the CD cavity. This finding implies that the solvophobic effect for the alkyl chain is necessarily stronger in water than in DMSO.

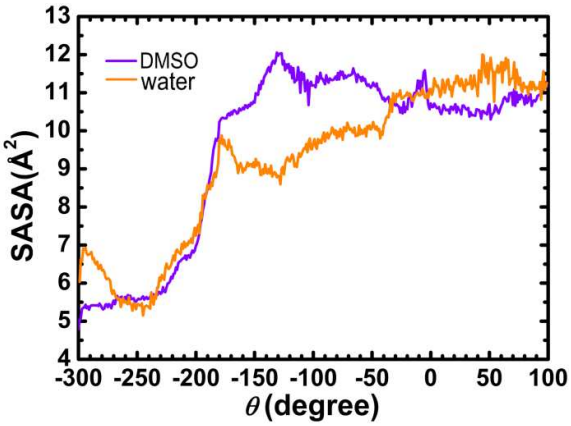

Fig. 10 Evolution of the SASA of the alkyl chain during tumbling, both in water and in DMSO.

Discussion

Hydrophobicity of the side chain. Since the hydrophobic effects of the chain plays a crucial role in the tumbling of the altropyranose unit, we suppose that apart from changing the solvent, modulation of the chain on its hydrophobicity can also control the occurrence of tumbling. To investigate the effect of the hydrophobicity on tumbling, we built a polyvinyl alcohol *altro*-α-CD model, which is very similar to the model of alkyl *altro*-α-CD except the highly hydrophilic chain (see Fig. 2A:**2**). The calculated free-energy profiles characterizing the tumbling of the polyvinyl alcohol *altro*-α-CD in water and DMSO are presented in Fig. 11B.

The PMF characterizing the tumbling of the polyvinyl alcohol *altro*-α-CD in water possesses two minima separated by a 27.1-kcal/mol free-energy barrier, and resembles that for the tumbling of the alkyl *altro*-α-CD in water. The activation free energy, however, has increased by 7.3 kcal/mol. The higher activation free energy after modification of the side chain can be ascribed in part to the hydrogen bonds formed between the hydroxyl groups of polyvinyl alcohol chain and water. Moreover, the conformational state of the non-included polyvinyl alcohol *altro*-α-CD (θ = +74°), which is 9.5 kcal/mol lower than its self-included counterpart (θ = −237°), corresponds to a thermodynamically stable state. The unstable self-included structure results from the desolvation of

the hydrophilic chain from bulk water, thus suggesting that tumbling is unlikely to occur in water upon replacement of the side chain by a hydrophilic one.

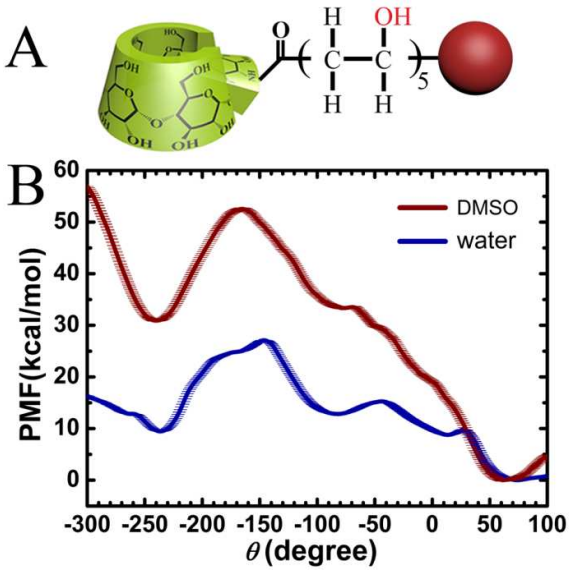

Fig. 11 (A) Schematic representation of tumbling the altropyranose unit of the polyvinyl alcohol *altro*-*α*-CD. (B) Free-energy profiles delineating the tumbling of the altropyranose monomer of the polyvinyl alcohol *altro*-*α*-CD in water and in DMSO, along the transition coordinate, θ, defined in Fig. 2. The error bars correspond to the statistical error of the free-energy calculation, i.e., the precision.

As can be observed in Fig. 11B, the free-energy profile characterizing tumbling of the polyvinyl alcohol *altro*-*α*-CD in DMSO is very similar to that determined in water, barring a significantly higher free-energy barrier. The self-inclusion structure arising from tumbling corresponds to a metastable state, indicating that tumbling would not occur in DMSO, with a more polar side chain. Furthermore, compared with the tumbling of the alkyl *altro*-*α*-CD in DMSO (Fig. 3B), tumbling of the polyvinyl alcohol *altro*-*α*-CD in DMSO requires that a higher free-energy barrier be overcome, which may be the consequence of hydrogen bonds formed between the polyvinyl alcohol chain and

the DMSO molecules.

Conclusion

The present contribution provides quantitative analysis of the activation free energy for the tumbling of an alkyl *altro*-*α*-CD in water and DMSO, as well as the relative thermodynamic stability of the inclusion complex. The strong exclusion of the hydrophobic alkyl chain from water contributes predominantly to the spontaneous tumbling of the altropyranose unit in the aqueous environment. The relatively strong hydrogen-bonding network within the CD and the propensity of DMSO molecules to bind to the rims of the CD results in a higher free-energy barrier in DMSO, compared to water. We initially anticipated that by increasing the hydrophilicity of the chain, tumbling would likely occur in DMSO. The calculations, however, indicate that this chemical modification prevents tumbling in water, but cannot trigger tumbling in DMSO. A possible explanation is that although DMSO is less polar than water, it is, nonetheless, a polar solvent. The polyvinyl alcohol chain is, therefore, expected to prefer the bulk DMSO, and its desolvation from a polar solvent is extremely unfavorable. It can be concluded that in addition to the polarity of the solvent, the hydrophobicity of the side chain also affects the frequency of tumbling. Furthermore, the propensity of the CD cavity to bind the chain is pivotal. Incorporation of a phenyl group at the proper site of the alkyl chain may significantly affect tumbling, in water, but also in DMSO. Overall, the spontaneous tumbling of the *altro*-*α*-CD derivatives can be controlled by the chemical and physical properties of the side chain, and the choice of the solvent.

Acknowledgements

This study is supported by National Natural Science Foundation of China (No. 21373117), MOE

Innovation Team (IRT13022) of China, and Natural Science Foundation of Tianjin, China (No. 13JCYBJC18800). The CINES, Montpellier, France, and NSCC, Tianjin, China, are gratefully acknowledged for provision of generous amounts of CPU time. The Cai Yuanpei program is also appreciatively acknowledged for its support of the international collaboration between the research groups of C.C. and W.C.

Notes and references

1 A. Harada, *Coord. Chem. Rev.*, 1996, **148**, 115–133.

2 K. K. Cotí, M. E. Belowich, M. Liong, M. W. Ambrogio, Y. A. Lau, H. A. Khatib, J. I. Zink, N. M. Khashab and J. F. Stoddart, *Nanoscale*, 2009, **1**, 16–39.

3 A. Coskun, M. Banaszak, R. D. Astumian, J. F. Stoddart and B. A. Grzybowski, *Chem. Soc. Rev.*, 2012, **41**, 19–30.

4 E. A. Neal and S. M. Goldup, *Chem. Commun.*, 2014, **50**, 5128–5142.

5 S. F. M. van Dongen, S. Cantekin, J. A. A. W. Elemans, A. E. Rowan and R. J. M. Nolte, *Chem. Soc. Rev.*, 2014, **43**, 99–122.

6 G. W. Gokel, W. M. Leevy and M. E. Weber, *Chem. Rev.*, 2004, **104**, 2723–2750.

7 C. Talotta, C. Gaeta, T. Pierro and P. Neri, *Org. Lett.*, 2011, **13**, 2098–2101.

8 R. Eelkema, K. Maeda, B. Odell and H. L. Anderson, *J. Am. Chem. Soc.*, 2007, **129**, 12384–12385.

9 S. Y. Dong, J. Y. Yuan and F. H. Huang, *Chem. Sci.*, 2014, **5**, 247–252.

10 G. Wenz, B. H. Han and A. Müller, *Chem. Rev.*, 2006, **106**, 782–817.

11 H. Murakami, A. Kawabuchi, R. Matsumoto, T. Ido and N. Nakashima, *J. Am. Chem. Soc.*, 2005, **127**, 15891–15899.

12 R. A. Bissell, E. Córdova, A. E. Kaifer and J. F. Stoddart, *Nature*, 1994, **369**, 133–137.

13 A. Coskun, D. C. Friedman, H. Li, K. Patel, H. A. Khatib and J. F. Stoddart, *J. Am. Chem. Soc.*,

2009, **131**, 2493–2495.

14 N. K. Jena and N. A. Murugan, *J. Phys. Chem. C*, 2013, **117**, 25059–25068.

15 C. J. Bruns and J. F. Stoddart, *Acc. Chem. Res.*, 2014, **47**, 2186–2199.

16 T. Da Ros, D. M. Guldi, A. Farran Morales, D. A. Leigh, M. Prato and R. Turco, *Org. Lett.*, 2003, **5**, 689–691.

17 K. Yamauchi, A. Miyawaki, Y. Takashima, H. Yamaguchi and A. Harada, *J. Org. Chem.*, 2010, **75**, 1040–1046.

18 K. Yamauchi, A. Miyawaki, Y. Takashima, H. Yamaguchi and A. Harada, *Org. Lett.*, 2010, **12**, 1284–1286.

19 Y. Liu, C. Chipot, X. G. Shao and W. S. Cai, *J. Phys. Chem. C*, 2014, **118**, 19380–19386.

20 J. C. Phillips, R. Braun, W. Wang, J. Gumbart, E. Tajkhorshid, E. Villa, C. Chipot, R. D. Skeel, L. Kalé and K. Schulten, *J. Comput. Chem.*, 2005, **26**, 1781–1802.

21 P. Liu, W. S. Cai, C. Chipot and X. G. Shao, *J. Phys. Chem. Lett.*, 2010, **1**, 1776–1780.

22 C. Cézard, X. Trivelli, F. Aubry, F. Djedaïni-Pilard and F. Y. Dupradeau, *Phys. Chem. Chem. Phys.*, 2011, **13**, 15103–15121.

23 S. J. Wallace, T. W. Kee and D. M. Huang, *J. Phys. Chem. B*, 2013, **117**, 12375–12382.

24 H. Y. Zhang, T. W. Tan, C. Hetényi, Y. Lv and D. van der Spoel, *J. Phys. Chem. C*, 2014, **118**, 7163–7173.

25 O. Guvench, S. N. Greene, G. Kamath, J. W. Brady, R. M. Venable, R. W. Pastor and A. D. MacKerell, *J. Comput. Chem.*, 2008, **29**, 2543–2564.

26 O. Guvench, E. Hatcher, R. M. Venable, R. W. Pastor and A. D. MacKerell, *J. Chem. Theory Comput.*, 2009, **5**, 2353–2370.

27 W. L. Jorgensen, J. Chandrasekhar, J. D. Madura, R. W. Impey and M. L. Klein, *J. Chem. Phys.*,

1983, **79**, 926–935.

28 M. L. Strader and S. E. Feller, *J. Phys. Chem. A*, 2002, **106**, 1074–1080.

29 S. E. Feller, Y. H. Zhang, R. W. Pastor and B. R. Brooks, *J. Chem. Phys.*, 1995, **103**, 4613–4621.

30 J. P. Ryckaert, G. Ciccotti and H. J. C. Berendsen, *J. Comput. Phys.*, 1977, **23**, 327–341.

31 H. C. Andersen, *J. Comput. Phys.*, 1983, **52**, 24–34.

32 T. Darden, D. York and L. Pedersen, *J. Chem. Phys.*, 1993, **98**, 10089–10092.

33 M. Tuckerman, B. J. Berne and G. J. Martyna, *J. Chem. Phys.*, 1992, **97**, 1990–2001.

34 W. Humphrey, A. Dalke and K. Schulten, *J. Mol. Graphics*, 1996, **14**, 33–38.

35 J. Comer, J. Phillips, K. Schulten, and C. Chipot, J. *Chem. Theor. Comput.*, 2014, **10**, 5276–5285.

36 J. Comer, J. C. Gumbart, J. Hénin, T. Lelièvre, A. Pohorille and C. Chipot, *J. Phys. Chem. B*, 2015, **119**, 1129–1151.

37 E. Darve and A. Pohorille, *J. Chem. Phys.*, 2001, **115**, 9169–9183.

38 E. Darve, D. Rodríguez-Gómez and A. Pohorille, *J. Chem. Phys.*, 2008, **128**, 144120.

39 J. Hénin and C. Chipot, *J. Chem. Phys.*, 2004, **121**, 2904–2914.

40 D. Rodríguez-Gómez, E. Darve and A. Pohorille, *J. Chem. Phys.*, 2004, **120**, 3563–3578.

41 C. Chipot and J. Hénin, *J. Chem. Phys.*, 2005, 123, 244906.

42 J. Hénin, G. Fiorin, C. Chipot and M. L. Klein, *J. Chem. Theory Comput.*, 2010, **6**, 35–47.

43 H. Flyvbjerg and H. G. Petersen, *J. Chem. Phys.*, 1989, **91**, 461–466.

44 D. Bucher, L. C. T. Pierce, J. A. McCammon and P. R. L. Markwick, *J. Chem. Theory Comput.*, 2011, **7**, 890–897.

45 M. Arrar, C. A. F. de Oliveira, M. Fajer, W. Sinko and J. A. McCammon, *J. Chem. Theory Comput.*, 2013, **9**, 18–23.